which are misinterpreted as charged-current events are not expected to populate the region $x > 0.1$. Thus the significance of the effect in the bin $x = 0.1-0.2$ does not depend on the assumed rate for neutral-current interactions in hydrogen. Within the statistical errors the effect shows no strong energy dependence.

We thank the members of the Neutrino Laboratory at Fermilab and the scanning and measuring staffs in our respective laboratories for their contribution to this experiment.

*Work supported by the U. S. Energy Research and Development Administration.

†Present address: CERN, Geneva, Switzerland.

‡Present address: Institute of High Energy Physics, Serpukhov, U. S. S. R.

§Present address: Institute of Theoretical and Experimental Physics, Moscow, U. S. S. R.

[1]B. C. Barish *et al.*, Phys. Rev. Lett. 31, 565 (1973).

[2]B. Aubert *et al.*, Phys. Rev. Lett. 33, 984 (1974).

[3]J. W. Chapman *et al.*, to be published.

[4]R. J. Cence *et al.* (University of Hawaii-Lawrence Berkeley Laboratory Collaboration), to be published.

[5]G. Myatt, CERN Report No. CERN/ECFA/72-4 (unpublished), Vol. II, p. 117.

[6]H. Burmeister and D. C. Cundy, CERN Report No. TC-L/Int. 75-1 (unpublished).

[7]C. H. Albright, Phys. Rev. D 8, 3162 (1973).

[8]A. Bodek, thesis, Massachusetts Institute of Technology, 1973 (unpublished).

Inclusive Cross Sections for 180° Production of High-Energy Protons, Deuterons, and Tritons in p-Nucleus Collisions at 600 and 800 MeV

S. Frankel and W. Frati
Department of Physics, University of Pennsylvania, Philadelphia, Pennsylvania 19174

and

O. Van Dyck and R. Werbeck
Clinton P. Anderson Meson Physics Facility, Los Alamos, New Mexico 87545

and

V. Highland
Department of Physics, Temple University, Philadelphia, Pennsylvania 19122
(Received 23 December 1975)

The inclusive cross sections, measured up to large values of effective mass ($\equiv q^2/2\nu$), are well fitted by $d\sigma/d^3p = B_x \exp(-\alpha_x p^2/2m_x)$. Values of B_x and α_x are given for Be, C, Cu, and Ta at the incident proton energy of 600 MeV and for Ag, Ta, and Pt at 800 MeV. Extremely large d/p and t/p ratios and large A and q^2 dependences of the relative cross sections are observed.

In order to examine the most violent p-nucleus interactions, with the hope of studying interactions with "correlated" nucleons or with "chunks" of nuclear matter, it is necessary to study the region of high effective mass, m^*, with $m^* \equiv q^2/2\nu$. (q^2 is the invariant momentum transfer and $\nu \equiv E_0 - E$ is the difference between the laboratory energies of the incident and scattered particle.) Measurement of high-q^2 events at low effective mass is a less effective probe of the coherent properties of nuclear matter. The high-q^2, high-m^* region has not hitherto been studied experimentally nor is there any theoretical guide to this region.

By working directly in a primary beam at the Clinton P. Anderson Meson Physics Facility (LAMPF) (10^{13} protons/sec), and by studying 180° production which maximizes q^2, we have been able to achieve sensitivities that have allowed, for example, observation of backscattered protons up to the high momenta corresponding to elastic backscattering from "clusters" with $A^* \equiv m^*/m_p = 6.5$ in Be^9. The measurements reported here were carried out simultaneously with a search for condensed nuclear states.[1]

This experiment utilized accelerator-beam-line equipment as the major part of our experimental apparatus. As shown in Fig. 1, protons passing through the LAMPF LB-BM-05 bending magnet struck targets mounted in a LAMPF remotely ac-

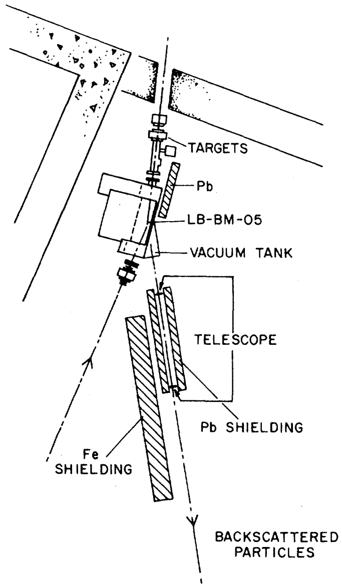

FIG. 1. Plan of experimental layout. Protons, deuterons, and tritons backscattered from targets just downstream of the C magnet are bent out through the fringe field into a time-of-flight scintillation-counter telescope. The momentum of the backscattered particle is varied by changing the telescope position.

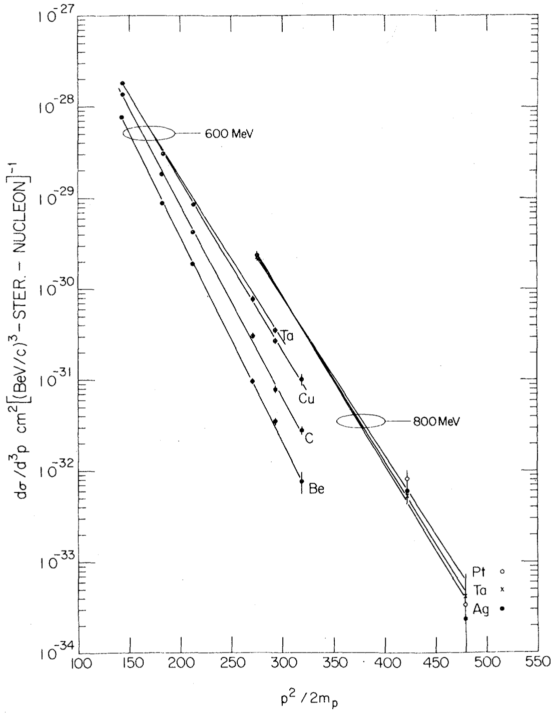

FIG. 2. Differential cross sections for 180° production of protons. The fits are made with $B_p \exp(-\alpha_p p^2/2m_p)$.

tivated scanning device. Secondary particles produced at 180° were bent out the side of the magnet through a 1-mil Havar window in the magnet vacuum chamber and passed through a scintillation-counter telescope composed of two scintillation-counter triplets separated by 1.8 m.[1] The LB-BM-05 magnet acted as our analyzing spectrometer with a momentum resolution of ~5% and an acceptance of $\sim 40\times10^{-6}$ sr. Protons, deuterons, and tritons were easily separated by measurement of times of flight in the telescope. dE/dx measurements clearly verified the p, d, and t assignments but with not quite as good precision as the time-of-flight separation. (Characteristic dE/dx and time-of-flight spectra are presented in Ref. 1.) The momentum of a backscattered particle was determined by the angle and position of the telescope, with a significant contribution to the uncertainty in our reported cross sections arising from positional inaccuracies ($\Delta p/p = \pm\frac{1}{4}\%$).

The yields of p, d, and t were obtained from the time-of-flight spectra, after subtraction of small backgrounds believed to be due to protons produced by neutrons striking the first scintillation counter and other upstream material. We were fortunate to be able to take a small portion of our data with a *chopped* incident proton beam so that comparison of time-of-flight spectra within our telescope with time-of-flight spectra from target to telescope allowed us to establish that backscattered particles were target-derived and did not originate in the magnet pole faces or vacuum chamber walls. A complete Monte Carlo simulation of our experiment, utilizing linear beam optics[2] for the dipole, and incorporating the effects of multiple scattering in the telescope and energy loss in both target and telescope, allowed us to extract differential cross sections from our yields and to fit our data with various theoretical distributions.

Figures 2–4 show plots of the differential cross sections $d\sigma/d^3p$ versus $p^2/2m_x$ with $x=p$, d, and t. The straight lines show our fits by the functional form $d\sigma/d^3p = B_x \exp(-\alpha_x p^2/2m_x)$. We emphasize that the exponential falloff dominates the the fit so that polynomial factors such as $B_x p^n \times \exp(-\alpha_x p^2/2m_x)$ with $n = \pm 1$ cannot be distinguished in this experiment from our choice of $n=0$ on the basis of χ^2. α_x is only mildly sensitive to n, with variations in n of ± 1 producing changes in α_x of less than 10–15%.

Figures 2–4 show the cross sections per nu-

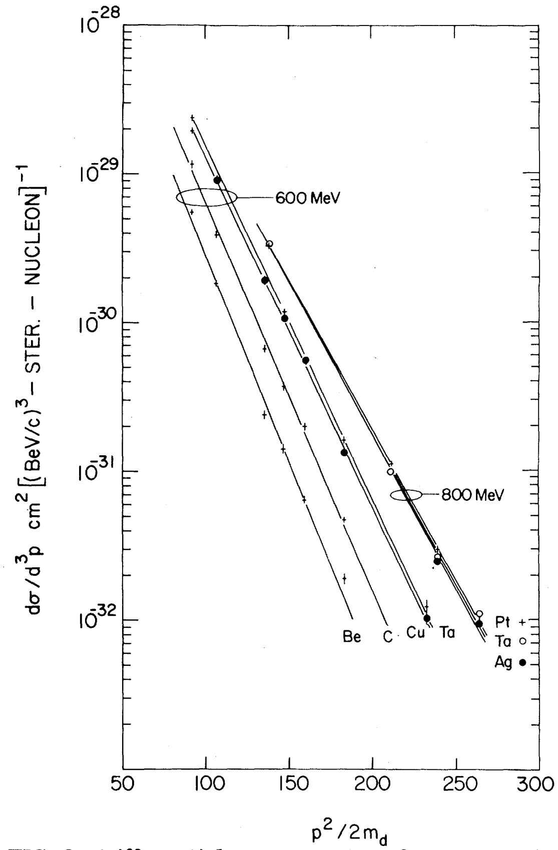

FIG. 3. Differential cross sections for 180° production of deuterons. The fits are made with $B_d \exp(-\alpha_d \times p^2/2m_d)$.

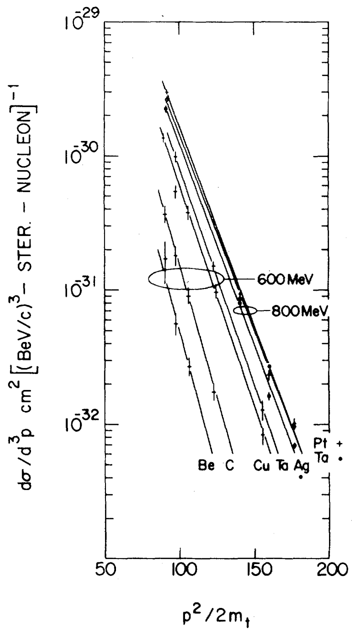

FIG. 4. Differential cross sections for 180° production of tritons. The fits are made with $B_t \exp(-\alpha_t p^2/2m_t)$.

cleon to demonstrate the nature of their A dependences. From these figures (and the data summary in Table I) we can conclude that (1) the differential cross sections fall off exponentially with p^2 and are fitted well by the functional form $B_x \exp(-\alpha_x p^2/2m_x)$; (2) there is a small A dependence of α_x; (3) there are large differences in the energy parameters α_x^{-1} for p, d, and t; (4) the differential cross sections increase with A in this region faster than A; (5) the A dependence favors large A more so at larger values of q^2; and (6) the A dependence is more marked for deuterons than for protons and for tritons than for deuterons.

Table I summarizes the values of B_x and α_x^{-1} for the 600- and 800-MeV data. The errors quoted include the statistical errors in the yields and an error introduced to simulate the momentum uncertainties introduced by the positional uncertainties in our spectrometer.[3]

TABLE I. Parameters resulting from the fit of the differential cross sections with the function $d\sigma/d^3p = B_x \times \exp(-\alpha_x p^2/2m_x)$. x represents protons (p), deuterons (d), or tritons (t). B_x is expressed in millibarns (BeV^3 sr nucleon)$^{-1}$, α_x^{-1} in MeV. Listed uncertainties reflect the statistical uncertainties in the yields and an assumed spectrometer momentum uncertainty of $\pm\frac{1}{4}$%. The absolute spectrometer calibration does not preclude a constant shift in α of up to 4%.

	600 MeV				800 MeV		
	Be	C	Cu	Ta	Ag	Ta	Pt
B_p	125±19	132±20	81±10	52±10	337±72	207±68	148±40
α_p^{-1}	19.2±0.3	20.5±3	23.3±0.3	24.5±0.6	23.2±0.4	24.1±0.7	24.8±0.5
B_d	1.67±0.27	2.21±0.31	2.74±0.30	3.43±0.45	2.24±0.36	1.97±0.31	1.81±0.28
α_d^{-1}	15.7±0.3	16.9±0.3	18.6±0.3	18.4±0.3	21.2±0.4	21.5±0.4	21.8±0.4
B_t	0.62±0.26	1.26±0.39	1.04±0.24	1.57±0.38	1.37±0.29	1.24±0.24	1.74±0.32
α_t^{-1}	10.6±0.5	11.0±0.4	13.2±0.4	13.3±0.4	14.3±0.3	14.9±0.3	14.4±0.3

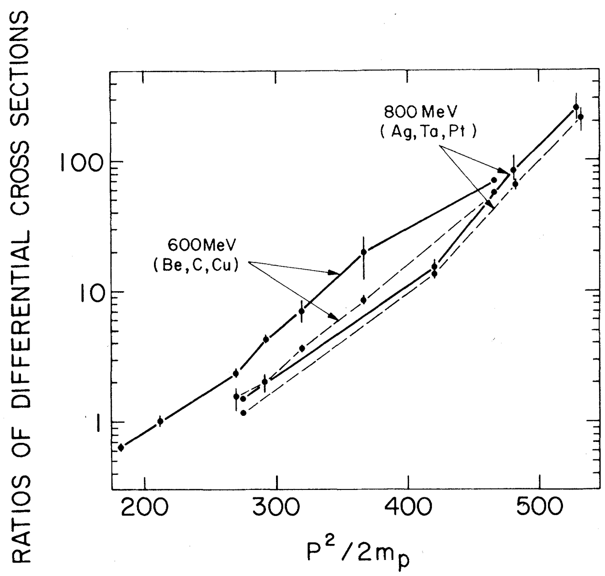

FIG. 5. Ratios of the differential cross sections for 180° production of deuteron and tritons relative to protons. The points represent the average values of the ratios for Be, C, and Cu at 600-MeV and Ag, Ta, and Pt at 800-MeV bombarding energy. The bars represent minimum and maximum values in each group of nuclei. Solid lines connect d/p ratios; dashed lines connect t/p ratios. The ratios are calculated for the same *momentum* and plotted versus $p^2/2m_p$.

Figure 5 shows the ratios of the differential cross sections (d/p and t/p) compared at the same measured *momentum*. For clarity the *average* value of each ratio is plotted for targets of different A. Be, C, and Cu are averaged for the 600-MeV data and Ag, Ta, and Pt are averaged for the 800-MeV data. The bars show the maximum *deviations* from the average. The low-energy triton and deuteron points include corrections for target energy loss so that ratios are compared at the same momenta. The fitted curves of Figs. 2–4 are employed for this correction. For the highest momentum point in both the 600- and 800-MeV data we have used our extrapolated proton cross sections but experimental d and t cross sections. These curves demonstrate (1) the very large d/p and t/p ratios that are observed at the same momentum in 180° production; (2) the relative independence of d/p and t/p on the nuclear species; (3) the near equality of the d and t cross sections over a very large d/p range; and (4) the fact (also seen in Table I) that the deuteron and triton cross sections have almost identical values of $\alpha_x/2m_x$.

The behavior of these differential cross sections at energies much greater than typical "Fermi" energies, and extending up to regions of $m^* \gg m_p$, shows an A dependence that may be characteristic of cooperative effects in the nucleus. Recently[4] similar effects have been found in the study of high-q^2 inclusive production of hadrons by 300-BeV protons. This Fermilab experiment shows less drastic A dependences, perhaps because it studies the nucleus at lower values ($m^* < m_p$) of the effective mass.

It would be particularly interesting to see how the form of the differential cross section changes as the region of the highest kinematically possible backscattered proton is approached, since extrapolation of our differential cross section predicts the feasibility of measurements of $q^2 = 8$ BeV^2 *elastic* scattering up to effective masses of $A^* \cong 20$.

We wish to thank the LAMPF accelerator staff for their cooperation and L. Shapiro for her programing assistance. We have enjoyed stimulating discussions of this physics with Professor R. D. Amado and Professor H. Primakoff. One of us (S. F.) wishes to thank CERN for its hospitality during part of the period when these data were being analyzed.

[1]S. Frankel, W. Frati, V. Highland, O. Van Dyck, and R. Werbeck, Phys. Rev. C 13, 737 (1976). The reader is referred to this paper for additional experimental details.

[2]We have incorporated the "Optik" program of T. J. Devlin, UCRL Report No. 9727, 1961 (unpublished), in our spectrometer simulation.

[3]The large errors in B_x arise from the strong correlations with the errors in α_x.

[4]J. W. Cronin, H. J. Frisch, M. J. Shochet, J. P. Boymond, P. A. Piroué, and R. L. Summer, Phys. Rev. D 11, 3105 (1975).